Vol. 06, No. 1 (2024) 419-430, doi: 10.24874/PES.SI.24.02.024

Proceedings on Engineering Sciences

www.pesjournal.net

ENHANCING MANUFACTURING EFFICIENCY WITH DYNAMIC FIREFLY-TUNED ADABOOST APPROACH FOR TALL BUILDING DESIGN

Ashuvendra Singh[1]
Sandeep Singh Rawat
Navneet Kumar

Received 10.11.2023.
Received in revised form 18.01.2024.
Accepted 24.01.2024.
UDC – 502.131.1

Keywords:

Tall Building Design, Manufacturing, Dynamic Firefly-Tuned AdaBoost (DFT-AdaBoost), Manufacturing Cost, Sustainability, Safety

A B S T R A C T

The planning of tall buildings is an important part of urban growth, and more and more attention is being paid to sustainability, safety, and efficiency in the building process. Traditional design and manufacturing processes frequently have trouble maximizing these factors, which results in inefficiencies and higher prices. This research introduces a revolutionary strategy that combines dynamic firefly tuned-AdaBoost (DFT-AdaBoost) in order to address the drawbacks of conventional tall building design methodologies. The goal is to increase manufacturing efficiency while also enhancing the tall building design's sustainability and safety features. The DFO is employed in an iterative manner to modify various design parameters, including material types, sizes, and shapes. On the other hand, AdaBoosting is utilized to improve the predicted accuracy of the model. The iterative nature of this methodology enables the ongoing improvement of design solutions in order to get the necessary level of manufacturing efficiency. The findings of this study indicate notable enhancements in manufacturing efficacy pertaining to the construction of tall buildings. The utilization of the DFT-AdaBoost method enables the identification of optimized design parameters, resulting in the reduction of material waste and a decrease in production costs. This study highlights the DFT-AdaBoost approach's potential as a potent tool for improving manufacturing effectiveness in tall building designs. This method contributes to the construction of tall buildings that are more cost-effective, safe, and environmentally responsible by integrating real-time structural optimization with manufacturing process prediction.

1. INTRODUCTION

Towering structures are outstanding examples of human creativity and ingenuity in the manufacturing sector. Relentlessly pursuing ever-higher verticality has resulted in the construction of famous skyscrapers that have completely changed urban landscapes and redefined our understanding of manufacturing efficiency. Tall building design, a multidisciplinary field bridging manufacturing, architecture, engineering, and sustainability, is critical to the realization of these enormous structures (Shen et al., (2018)). In-depth

[1] Corresponding author: Ashuvendra Singh
Email: Pc.ce@dbuu.ac.in

coverage of the complex field of tall building design from a manufacturing standpoint is provided in this introduction, together with information on its historical development, vital position in modern urban planning, and cutting-edge tactics influencing its further development.

1.1 An Overview of Historical Context

The notion of building enormous constructions has always captivated mankind. Throughout history, numerous societies have attempted to reach unprecedented heights; examples include the magnificent pyramids of Egypt, the opulent Gothic cathedrals of Europe, and the ancient ziggurats of Mesopotamia (Elias et al., (2018)). But the start of the Industrial Revolution in the late 19th century marked a turning point in the development of tall building design. This period saw a revolutionary change in manufacturing due to improvements in steel production and building methods. From an aerial perspective, these inventions not only made it easier to build skyscrapers but also completely changed the urban environments of big cities like New York, Chicago, and London (Tomei et al., (2018)).

The Woolworth Building by Cass Gilbert and the famous Flatiron Building in New York City by Daniel Burnham were two pioneering examples of the buildings that sparked the history of tall building design from a manufacturing aspect. The industrial procedures involved in the creation of these architectural wonders were changed, in addition to redefining the skyline. A new era of manufacturing techniques was ushered in by them, and this inspired architects and engineers to push the limits of what was possible in the creation of towering buildings (Pan et al., (2020)).

1.2 Tall Buildings in Modern Environment

The 21st century has witnessed a notable increase in the rate of urbanization. Greater demand for vertical living and working spaces has resulted in people moving more and more to cities in search of employment prospects. As a result of their designs changing to meet various problems, tall buildings are no longer the exception but rather the rule. According to Ji et al. (2017), sustainability in the manufacturing sector becomes the most important factor to take into account when planning and constructing modern tall buildings. Their impact on the environment, including material and energy usage, is being closely examined in relation to these towering constructions. Using cutting-edge methods like green roofs, renewable energy, and high-tech insulation materials, architects and engineers are lowering the carbon footprint of these massive structures. This is done from a manufacturing aspect. According to Li et al. (2018), creating resilient, livable, and environmentally conscious urban ecosystems is a critical goal in the pursuit of sustainability, which goes beyond energy efficiency alone.

1.3 Architectural Creativity and Aesthetics

Tall buildings represent a city's personality and aspirations and go beyond just practical constructions from a manufacturing aspect. As such, design is heavily influenced by aesthetics. Creating unique, eye-catching monuments that improve the urban environment is the goal of architects. Elshaer et al., (2017) cite the Shanghai Tower and the Burj Khalifa as two architectural marvels designed by Adrian Smith and Jun Xia that demonstrate the harmonious combination of mechanical expertise and artistic vision to create world-famous skyscrapers. Furthermore, "vertical communities" are becoming more and more popular in the context of developing towering structures. More than just places to work or live, these structures are linked ecosystems that support residents' sense of well-being and belonging. Facilities like sky gardens, social areas, and mixed-use developments are being incorporated more and more into the manufacturing of tall buildings in order to promote a feeling of community amidst extreme heights (Li et al., (2017)).

1.4 Engineering Innovations and Structural Difficulties

In order to meet certain obstacles, the manufacturing of tall structures must adopt modern technical solutions. Because of wind loads, seismic activity, and the sheer height of these structures, innovative manufacturing solutions are required. Modern production techniques, advanced computer-aided design and manufacturing systems, and advanced materials are used by manufacturers to guarantee the quality and safety of towering construction components. According to Oh et al. (2017), cooperation between engineering and manufacturing teams is crucial because their combined knowledge results in components that push the limits of what is technically possible.

1.5 Future Tall Building Design: A Look Ahead

Tall building manufacturing is always changing in response to trends in urbanization, advances in technology, and environmental concerns. Ideas like self-sufficient skyscrapers, vertical forests, and even the incorporation of spaceports into these enormous buildings are what are next. The integration of artificial intelligence and the progression toward "smart cities" have the potential to significantly transform the manufacturing, management, and upkeep of tall buildings (Micheli et al., (2020)).

1.6 Key Contributions

- The study presents a new methodology, referred to as Dynamic Firefly-Tuned AdaBoost (DFT-AdaBoost), as a means to overcome the constraints associated with traditional approaches in tall structure design.

- The research intends to optimize design factors such as material types, sizes, and shapes by iteratively utilizing the DFT-AdaBoost approach. Sustainable building practices necessitate minimizing construction waste, which can be achieved through optimization.
- The study highlights the significance of manufacturing efficiency in the construction of tall buildings.
- The reduction in manufacturing cost is listed as one of the tangible benefits. The determination of optimal design parameters leads to this cost savings.
- The data set pertaining to a 35-storey structure was gathered, followed by a thorough analysis that encompassed several parameters like accuracy, manufacturing cost, drift ratio, demand-capacity ratio, and the strength-to-weight (SC/WB) ratio.

The rest of this article is divided into the following sections: Section 2, Related Works; Section 3, The Optimal Problem Statement; Section 4, Enhancing Manufacturing Efficiency for Tall Building Design (Methodology); Section 5, Result; and Section 6, Conclusion.

2. RELATED WORKS

In this section, we provide a summary of existing research studies that focus on the analysis of methods to improve manufacturing efficiency in the construction of tall buildings.

Elshaer et al. (2017) introduced a process for optimizing the aerodynamics of building corners, known as the Building Corner Aerodynamic Optimization process (AOP). The objective of their procedure was to minimize wind load by integrating three key components: an optimization algorithm, large eddy simulation (LES), and an artificial neural network (ANN) based surrogate model. Meng et al. (2018) aimed to conduct a comprehensive assessment of the changes in wind pressure coefficients among CAARC standard tall buildings through the use of computational fluid dynamics (CFD) simulations. To analyze and describe the patterns of wind pressure distribution over CAARC models, focusing on four distinct wind directions. Gan et al. (2017) evaluated and investigated the amount of embodied carbon present in tall buildings, taking into consideration many design factors such as construction material selection, incorporation of recycled materials, structural configurations, and building heights. Petrini et al. (2020) presented an innovative approach to designing an optimal Tuned Mass Damper and Inerter (TMDI) system. The objective was to enhance occupants' comfort in tall buildings that were vulnerable to the effects of vortex shedding caused by wind. Additionally, it investigated the potential of the optimal TMDI system in converting a portion of the wind-induced kinetic energy into usable electricity within tall buildings. Cruz and Miranda (2017) established the appropriate damping ratios that should be utilized in the seismic analysis of high-rise buildings. This was achieved by the application of linear elastic modal analysis and a fixed-base model, with the intention of accurately replicating the observed responses.

Gan et al. (2018) created a comprehensive Building Information Modeling (BIM) framework that can effectively assess and discern environmentally friendly low-carbon designs for tall buildings. The methodology that has been suggested possesses the capability to quantitatively assess and mitigate the embodied carbon emissions associated with construction materials, as well as the operational carbon emissions resulting from the energy consumption of buildings during their lifespan. Venanzi et al. (2018) introduced a theoretical framework for estimating life-cycle losses associated with non-structural damage in tall buildings subjected to wind and seismic stresses. The findings also indicated that wind load faces greater expenses in terms of damages caused by drift-dependent factors compared to seismic load. De Domenico et al. (2020) examined the seismic response of interconnected high-rise buildings fitted with an innovative MTMDI technology. An actual case study involving two high-rise buildings connected by a horizontal corridor has been used to perform based on performance optimization of MTMDI parameters utilizing a suite of 44 ground motion data from the FEMA P695 far-field record collection, each of which contains unique frequency content. Liew et al. (2019) examined the design and construction obstacles encountered in the implementation of modular construction techniques for high-rise buildings and proposed potential resolutions to address these issues. A study presented the introduction of a unique steel-concrete composite technology designed to effectively decrease the overall weight of the module while maintaining its structural integrity and rigidity. Ierimonti et al. (2017) presented an innovative method for Life Cycle Cost Analysis (LCCA) that builds upon the existing seismic engineering strategy. The proposed methodology aimed to assess the likelihood of non-structural damage and predict maintenance expenses for tall buildings. To achieve this, the methodology incorporates data on aerodynamic loads obtained from wind tunnel experiments conducted on a scaled-down model.

Gan et al. (2017) established a methodology for the measurement and evaluation of the carbon footprint associated with tall structures. The findings of their study provided evidence for the development of a sustainable material procurement strategy aimed at mitigating the embodied carbon emissions associated with the construction industry. Tong et al. (2017) presented an initial attempt to comprehend and predict the vertical patterns of nighttime visibility (NV) in prominent cities across six climate zones in the United States. That was achieved by employing an internally developed atmospheric boundary layer (ABL) meteorology model. Lu et al. (2017) introduced a novel damping device, referred to as the Particle-Tuned Mass Damper (PTMD), which combines the principles of the standard Tuned Mass Damper (TMD) and particle damper. The impacts of wind-

induced vibration control on high-rise buildings were comprehensively examined by an aero-elastic wind tunnel test. Ghazali et al. (2017) evaluated the viability of implementing a vertical photovoltaic system on a high-rise structure in Malaysia, with a specific emphasis on assessing its efficacy and conducting an economic evaluation. Weerasuriya et al., (2019) introduced a comprehensive BIM framework that assesses the natural ventilation capabilities of a 40-storey residential structure. The structure integrated Computational Fluid Dynamics (CFD) simulation, Building Energy Simulation (BES), and multi-zone-air-flow-modelling techniques.

3. PROBLEM STATEMENT

The following describes the general formula for optimizing seismic design in tall buildings. Traditional load and resistance factor design (LRFD) is used for the structural design process:

3.1 Design for Serviceability

According to the Canadian for Seismic Resistant Design of Buildings (Standards Association (CSA) S16), the following limitation must be met under design seismic forces for buildings that are more than five storeys high:

$$D_c \Delta_j \leq 0.02 \tag{1}$$

Where D_c denotes the amplifying factor responsible for the anticipated inelastic response

3.2 Design for strength

In accordance with the regulations outlined in the building code, it is imperative that the demand-capacity ratio, as specified in Equation (2), remains at or below a value of one for any load combination.

$$\frac{Q_v}{\phi\, Q_m} \leq 1 \tag{2}$$

Where,
$\phi\, Q_m$ denotes the design strength of every structural member and
Q_v denotes the necessary strength for every combination of LRFD loads.

3.2 SC and WB

In the construction of "Special Moment Frames (SMFs)," it is necessary for the moment ratio to meet the specified criteria at every connection point between a beam and a column.

$$\frac{\sum N_{oa}^{*}}{\sum N_{od}^{*}} < 1 \tag{3}$$

Where,
$\sum N_{od}^{*}$ denotes the columns' overall flexural strength when the axial force is reduced, and
$\sum N_{oa}^{*}$ denotes the total flexural strength of all beams attached to the connection.

3.4 Practical restrictions

Column sizes on lower floors shouldn't be smaller than those on higher floors for practical reasons. It is possible to express this limitation as:

$$c_{i,j}^{col} \geq c_{i+1,j}^{col},\ a_{i,j}^{col} \geq a_{i+1,j}^{col},\quad i = 1,2,\cdots,NS-1;\quad j = 1,2,\cdots,NC, \tag{4}$$

The vertical and horizontal dimensions of the section of the j^{th} column on the i^{th} level are denoted by $c_{i,j}^{col}$, and $a_{i,j}^{col}$ in Equation (4). The number of columns in each narrative is denoted by NC, and the total number of stories is denoted by NS.

The objective function in the present design optimization problem pertains to the cumulative weight of the beams and columns within the three-dimensional steel high-rise structure. The inequalities indicated above are utilized as constraints for optimization. Furthermore, the design criteria are applicable to the section properties of the structural components. The present study employs two fundamental methodologies to address the ensuing nonlinear restricted optimization problem.

The initial technique under consideration is the meta-heuristic optimization approach known as DFA. The second strategy involves the utilization of the AdaBoost method to ascertain nonlinear inequality constraints, as opposed to employing analytical methods that are more time-consuming.

4. ENHANCING MANUFACTURING EFFICIENCY FOR TALL BUILDING DESIGN

DFT-AdaBoost streamlines manufacturing procedures by optimizing structural design criteria for tall buildings. It improves structural efficiency by utilizing adaptive algorithms, cutting down on wasteful material usage and building time. This ground-breaking strategy transforms the architecture of towering buildings while guaranteeing economical and environmentally responsible construction. Figure 1 displays the overview of the tall building design.

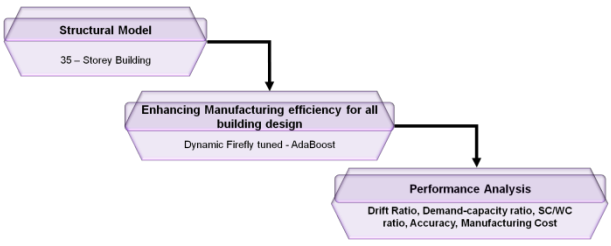

Figure 1. Enhancing manufacturing efficiency for tall building design

4.1 Model of Structure

The subject of analysis is a steel office building situated in San Francisco, California, which stands at a height of 35 stories (Wang and Mahin, (2018)). The dimensions of the tower are approximately 56 meters x 41 meters in plan, with a height of 150 meters. Both the vertical and horizontal axes of the structural system are supported by fully three-dimensional moment-resisting space frames. Figure 2 depicts the architectural plan of the building, including the standard floor height and bay widths. Prior to the Northridge earthquake, beam-to-column moment connections had their signature features, while partial penetration welds were used primarily in the column slice details. Both types of data are extremely sensitive.

All above-ground parts of the structure were accounted for in the virtual representation. It was assumed for the purposes of this study that the ground-level boundary condition was a fixed base. Nonlinear beam-column components, based on displacement, were used to simulate the columns; these included “fiber sections and the Giuffré-Menegotto-Pinto material model (Steel02).” The assessment was conducted under the assumption that the old building's column splices, which made use of partial joint penetration welds, were replaced with full welds.

The floor plans of this building are depicted in Figure 2, representing the standard layout. The layout is composed of six bays, each measuring 4 meters in length, as observed in both directions. The perimeter tube of the structure is composed of box sections for both the gravitational columns (RC) and the corner columns (OC). The remaining columns, namely E1C and E2C, are constructed using I-shaped sections. According to the information presented in Figure 2, there exist two distinct categories of non-corner perimeter columns. The initial classification, denoted as E1C columns, is exclusively linked to the perimeter beams on both sides. The second type, referred to as E2C columns, is also associated with the pin-ended gravitational beams (RB). The spandrel beams, denoted as SB, are characterized by fixed-ended supports and possess a length of 4 meters. Furthermore, it should be noted that both gravitational beams, namely RB and IRB, possess pin-ended configurations and have a uniform length of 8 meters. As depicted in Figure 2, IRB beams serve the purpose of linking the gravitational columns, whereas GB beams are responsible for connecting the gravitational columns to the perimeter tube.

Force-based nonlinear beam-column elements with finite-length plastic hinges at both ends were used to simulate the beams. The moment-curvature relationship of the beams was deemed "brittle" when a hysteretic material model was applied to it. The constructed model incorporated constraints on the upper and lower bounds of rotational capabilities in accordance with the regulations specified in ASCE 41. The design lacks the inclusion of panel zones, the perimeter precast concrete façade, as well as non-constructional components like elevator core walls and changeable interior partitions. The first three elastic modal periods of the structure, which involved retrofits at Level-1, were found to be 4.33 seconds for translation in the X-direction, 4.18 seconds for translation in the “Y-direction, and 3.59 seconds for rotation.”

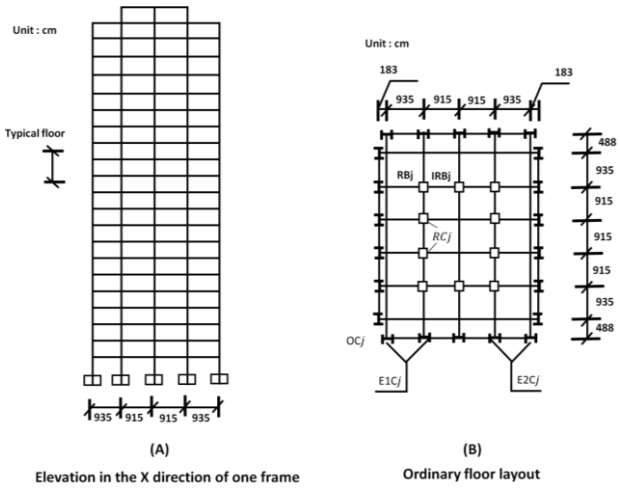

Figure 2. Illustration of the model building

4.2 Decision Variables

This study examines the continuous nature of the decision variables in relation to the sections' attributes. The quantity of design variables significantly decreases by establishing rational equations that establish a relationship between the dimensions of the section and its depth. This study aims to establish linear equations that establish the relationship between the dimensions of sections and their depths based on Dolor-standard sections. Equations (5) and (6) illustrate the relevant mathematical expressions that govern the behavior of I-shape sections in the non-corner columns of the perimeter tube and beams.

$$\begin{aligned} a_e &= c, \\ s_e &= 0.056c + 0.36 \\ s_x &= 0.016c + 0.7 \end{aligned} \tag{5}$$

$$\begin{aligned} a_e &= 0.36c + 3.4, \\ s_e &= 0.027c + 0.34 \\ s_x &= 0.017c + 0.26 \end{aligned} \tag{6}$$

Equations (5) and (6) define the variables used in the analysis. Within this particular context, the variable c is utilized to represent the section depth, a_e is employed to signify the flange width, s_e is utilized to represent the flange thickness, and s_x is employed to designate the web thickness.

As already mentioned, the corners and gravitational columns are characterized by portions with a box shape.

The Equation that describes the relationship between the width (s) of the box section and its depth (c) is stated as follows.

$$s = 0.06 \quad (7)$$

4.3 Dynamic Firefly Optimization (DFO)

In comparison to other metaheuristics, the DFO has been demonstrated to perform better; nonetheless, it is not without its restrictions and has a threshold. The parameters of the model are predetermined and demonstrate efficacy when applied to functions with limited dimensions and a small number of variables. Initial fixed-value parameters may be inappropriate in optimization scenarios with many design variables and design constraints, reducing the effectiveness of the method. Figure 3 displays the general flow of dynamic firefly optimization.

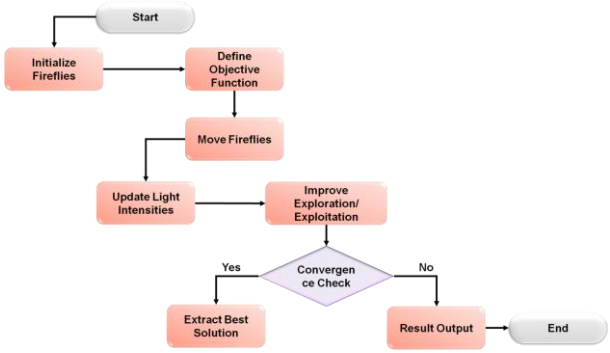

Figure 3. Dynamic Firefly optimization

In small-scale optimization problems with a limited number of design variables, the closeness of fireflies is an important metric, and the parameter is meaningful. In contrast, while dealing with high-dimensional and large-sized issues, the proximity of neighboring fireflies becomes very remote, leading to a reduction in the value of β. The efficiency of the algorithm is notably inadequate, particularly when dealing with optimization issues of significant scale, due to the direct correlation between attractiveness and firefly brightness. Therefore, in order to address this disparity, the subsequent methodology for improving attractiveness is presented in Equation (8).

$$\beta(q) = (\beta_0 - \beta_{min}) * f^{\left(-\gamma_{(iter)} q^2_{normalized}\right)} + \beta_{min} \quad (8)$$

Where,

β_0 Represents the level of attractiveness of the firefly in its initial location and is assigned a value of 1.0.

The value of β_{min}, representing the minimal attractiveness of the firefly, is set at 0.1, a rather tiny magnitude.

The term $q_{normalized}$ refers to the distance that has been normalized.

γ_{iter} Represents the increased absorption coefficient

The values were determined and established using Equations (9) and (10) as the respective calculation and definition methods.

$$q_{normalized} = \frac{q_{ji}}{q_{max}}$$

Where,

$$q_{ji} = \sqrt{\sum_{l=-1}^{mh} \left(Sect_j^l - Sect_j^l\right)^2} \; and \; q_{max} = \sqrt{\sum_{l=1}^{mh} (LimitUpsect - LimitLowSect)^2} \quad (9)$$

$$\gamma_{(iter)} = \gamma_{max} - \left[\left(\sqrt{\frac{iter}{iter_{max}}}\right) * (\gamma_{max} - \gamma_{min})\right] \quad (10)$$

Where,

The variable γ_{iter} represents the current value of the absorption coefficient, $iter$.

The absorption coefficient values, γ_{max}, and γ_{min}, are defined in the method as the maximum and minimum values, respectively.

$iter_{max}$ is the upper limit for the number of iterations during which the tolerance minimization operation is executed.

Equation (10) guarantees that the absorption coefficient values are initially higher during the early stages of the design cycles and gradually decrease towards the later stages of the design cycles. In this manner, the value of γ is dynamically modified based on Equation (10), which is initially established at the commencement of the conventional algorithm and remains constant during the search process.

The primary rule entails the implementation of a proficient algorithm that possesses the ability to effectively balance its exploration and exploitation skills. The algorithm's capacity to explore enables it to avoid being confined to a local optimum by doing a comprehensive search of the whole solution space. Therefore, the act of flying in a random manner enables the firefly to engage in a more comprehensive and investigative search, thereby facilitating its ability to navigate to novel and potentially distant areas within the search environment. In addition, a local search strategy aims to utilize the search process further. The proposed method involves perturbing a firefly sample taken from the existing population near its current solution. This disruption facilitates the firefly's exploration of adjacent locations, potentially impeding the convergence of fireflies towards the global optimum.

A comparable formulation is applied to the randomness parameter (α) as described in Equation (11) in order to achieve a wide exploration of the search space. This is accomplished by assigning a higher value to α, particularly in the initial stages, and gradually decreasing its value in the later stages to facilitate improved convergence.

$$\alpha_{(iter)} = \alpha_{max} - [\left(\sqrt{\frac{iter}{iter_{max}}}\right) * (\alpha_{max} - \alpha_{min})] \quad (11)$$

Where,
The value of the randomness parameter, denoted as α_{iter}, represents the value of the randomness parameter in the $iter$.

The variables α_{max} and α_{min} are the upper and lower bounds of the randomness parameter values that are specifically defined within the method.

$iter_{max}$ represents the maximum number of iterations at which the tolerance minimization operation will proceed.

Fireflies exhibit a behavior known as improvising of movement, wherein they select new parts and develop new designs. This phenomenon can be described using Equation (12).

$$Sect_j^l = Sect_j^l + \beta(q) * \left(Sect_i^l - Sect_j^l\right) + \alpha_{(iter)} * (rand - 0.5) \quad i,j = (1,2,\dots,m)\ and\ l = ((1,2,\dots,mh) \tag{12}$$

Where,
The variable "$Sect_j^l$" the numerical value, denotes the specific part of the profile chosen by the firefly "j" for the "l^{th}" firefly.

The function $\beta(r)$ represents the improved attractiveness method.

The variable α_{iter} represents the modification of the randomness parameter.

The variable "$rand$" represents a random number generator that follows a uniform distribution inside the interval [0,1].

Upon the completion of the movements of all fireflies, one cycle is concluded.

4.4 Adaptive Boosting (AdaBoost)

The AdaBoost algorithm is commonly referred to as Adaptive Boosting. AdaBoost is a meta-algorithm that involves training many weak classifiers using a training set and afterward combining them to create a strong classifier. The weak classifier, represented as $g(w,e,o,\theta)$, is composed of a feature (e), a threshold (θ), and a polarity (o) that determines the direction of the inequality.

$$g(w,e,o,\theta) = \begin{cases} +1\ if\ oe(w) < o\theta \\ -1\ otherwise \end{cases} \tag{13}$$

A robust AdaBoost classifier can be constructed using the linear aggregation of many weak classifiers, with each weak classifier assigned its own weight. During the training phase of AdaBoost, the error rate of each weak classifier is observed in each iteration and subsequently modified. The weak classifiers that exhibit lower mistake rates are assigned greater weights in the linear combination. Furthermore, it is worth noting that each training sample possesses its own individual weight. The misclassified samples are assigned larger weights, which encourages weak classifiers to prioritize their correct classification in subsequent iterations. The AdaBoost training method is characterized by a comprehensive and intricate description. Initially, a collection of training instances is taken into account, encompassing both affirmative and negative instances. The positive samples are denoted by the label +1, whereas the negative samples are denoted by the label -1, as represented by the following expression:

$$T = (w_1,z_1),(w_2,z_2),(w_3,z_3),\dots\dots,(w_n,z_n), w_j \in W, z_j \in \{1,-1\}. \tag{14}$$

Additionally, the weights of each training sample are initialized. Given the absence of initial error rate information, equal weights are assigned to each of the samples. The process of initialization is carried out in the following manner:

$$C_1(j) = \frac{1}{n}, j = 1,\dots,n \tag{15}$$

Where,
The variable $C_1(j)$ represents the weight assigned to the sample i during the initial iteration.

Next, the training process commences iteratively. We employ S iterations corresponding to the S weak classifiers being evaluated. This can be formulated as an optimization problem.

$$For\ s = 1,\cdots,S, find\ a\ classifier$$
$$g_s: W \longrightarrow \{-1,+1\} \tag{16}$$

This aims to minimize the error in relation to the variable C_s, that is

$$g_s = \arg\min_{g_i} \varepsilon_i \tag{17}$$

Where

$$\varepsilon_i = \sum_{j=1}^{n} C_s(j)\left[z_j \neq g_i(w_j)\right] \tag{18}$$

The term g_j is indicative of a classifier that possesses little strength.

During each cycle, the weights of the weak classifiers are adjusted by a specific process.

$$\alpha_s = \frac{1}{2} 1m \frac{1-\varepsilon_s}{\varepsilon_s} \tag{19}$$

Additionally, in order to provide misclassified samples with a greater opportunity for learning, the distribution of the samples is modified in each iteration by:

$$C_{s+1}(j) = \frac{C_s(j)\exp\left[-\propto_s z_j g_s(w_j)\right]}{Y_s} \tag{20}$$

Where,
The variable Y_s is employed for the purpose of normalization.

Ultimately, the construction of a robust classifier $G(W)$ can be achieved by:

$$sign\ (G(w) = \sum_{s=1}^{S} \propto_s g_s(w)) \tag{21}$$

4.5 Dynamic Firefly-Tuned AdaBoost (DFT-AdaBoost)

DFT-AdaBoost is a cutting-edge strategy that could revolutionize the production effectiveness of tall building designs. Algorithm 1 describes the DFT-AdaBoost algorithm. Building design and construction are frequently difficult, time-consuming operations in the field of architectural engineering. This ground-breaking approach combines the strength of two cutting-edge algorithms, Dynamic Firefly optimization, and AdaBoost, to handle the unique difficulties presented by tall structure design.

The most effective method for finding the ideal design parameters is called DFT, which takes its name from the swarming activity of fireflies. This program allows for the exploration of a large design area in search of the most effective and structurally sound solutions by imitating the way that fireflies communicate and change their brightness to attract mates. The design process may be continuously adjusted and fine-tuned thanks to its dynamic character, which guarantees that it is responsive to shifting restrictions and requirements. The machine learning ensemble technique AdaBoost, on the other hand, is exceptional at classification tasks. It can be used to examine and improve a number of factors, including energy effectiveness, structural integrity, and environmental impact, in the context of designing tall buildings. AdaBoost is integrated into the system so that it may learn from previous data and make decisions based on that knowledge throughout the design process, ultimately producing more sustainable and energy-efficient tall structures.

In this hybrid approach, the interaction of DFT-AdaBoost enables architects and engineers to greatly increase manufacturing efficiency. It makes it possible to quickly produce creative design solutions that are tailored to fulfill both functional and sustainability objectives. In the end, this technology has the ability to lower construction costs, accelerate project completion, and aid in the creation of iconic tall structures that are not only visually appealing but also environmentally friendly.

Algorithm 1: Dynamic Firefly-Tuned AdaBoost (DFT-AdaBoost)

Step 1: Initialize design parameters and data

Step 2: Initialize fireflies randomly

Step 3: Initialize the AdaBoost ensemble

Step 4: Set maximum iterations or convergence criteria

Step 5: While not converged or maximum iterations not reached:

Step 6: Evaluate the fitness of each firefly based on design parameters

Step 7: Update the brightness of fireflies based on fitness

Step 8: Perform AdaBoost ensemble learning on the current design parameters

Step 9: Update the design parameters based on AdaBoost predictions

Step 10: End While

Step 11: Select the best design parameters found

Step 12: Output the optimized tall building design

5. PERFORMANCE ANALYSIS

This section provides a thorough examination of the best configurations and seismic behavior of the 35-storey framed tube system. The optimization process for the 35-storey structure involves a total of 44 decision factors. The depths of the sections in the ideal designs linked to the 35-storey structure, including both systems.

The concept of "drift ratio" within the realm of tall building design predominantly relates to the field of structural engineering and holds significant importance in guaranteeing the security, stability, and effectiveness of lofty edifices, such as skyscrapers. The drift ratio is a metric used to quantify the horizontal displacement or movement encountered by a structure during dynamic occurrences such as wind-induced forces or seismic events. The ratio of a point's lateral displacement, also known as drift, to that point's height above the structure's base, is known as the drift ratio. Table 1 and Figure 4 illustrate the inter-storey drift ratios pertaining to the optimal design considerations for the 35-storey building.

$$Drift\ Ratio = \frac{Lateral\ Displacement}{Height} \tag{22}$$

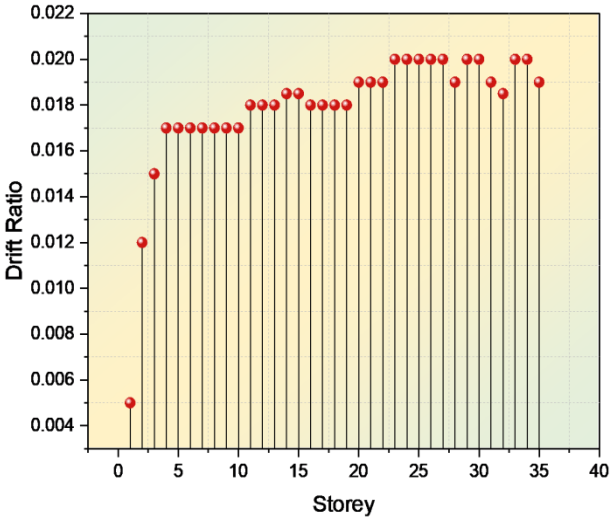

Figure 4. Drift Ratio for 35-Storey Building

Table 1. Drift Ratio for 35-Storey Building

Storey	**1**	**2**	**3**	**4**	**5**	**6**	**7**	**8**	**9**	**10**
Drift Ratio	0.005	0.012	0.015	0.017	0.017	0.017	0.017	0.017	0.017	0.017
Storey	**11**	**12**	**13**	**14**	**15**	**16**	**17**	**18**	**18**	**20**
Drift Ratio	0.018	0.018	0.018	0.0185	0.0185	0.018	0.018	0.018	0.018	0.019
Storey	**21**	**22**	**23**	**24**	**25**	**26**	**27**	**28**	**29**	**30**
Drift Ratio	0.019	0.019	0.02	0.02	0.02	0.02	0.02	0.019	0.02	0.02
Storey	**31**	**32**	**33**	**34**	**35**	-				
Drift Ratio	0.019	0.0185	0.02	0.02	0.019					

In urban planning and civil engineering, the demand-capacity ratio (DCR) is a widely used concept, especially in relation to zoning and building rules. It assists in ascertaining whether the planned construction or development project complies with regional zoning laws and regulations. The DCR is determined by contrasting the capacity of specific resources or services that are available locally with the demand for those resources or services that are produced by a project. Table 2 and Figure 5 illustrate the inter-storey Demand-capacity ratio pertaining to the optimal design considerations for the 35-storey building.

$$DCR = \frac{Demand\ for\ tall\ building\ manufacturing}{capacity} \quad (23)$$

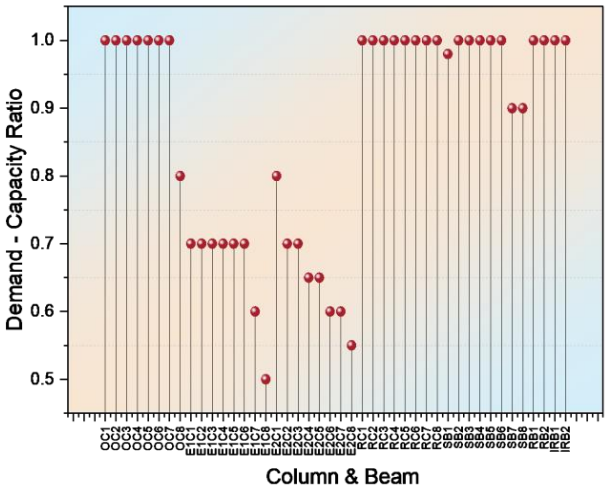

Figure 5. Demand-capacity ratio for 35 Storey Building

Table 2. Drift Ratio for 35-Storey Building.

Column & Beam (OC)	**1**	**2**	**3**	**4**	**5**	**6**	**7**	**8**
Demand - Capacity Ratio	1	1	1	1	1	1	1	0.8
Column & Beam (E2C)	**1**	**2**	**3**	**4**	**5**	**6**	**7**	**8**
Demand - Capacity Ratio	0.8	0.7	0.7	0.65	0.65	0.6	0.6	0.55
Column & Beam (E1C)	**1**	**2**	**3**	**4**	**5**	**6**	**7**	**8**
Demand - Capacity Ratio	0.7	0.7	0.7	0.7	0.7	0.7	0.6	0.5
Column & Beam (RC)	**1**	**2**	**3**	**4**	**5**	**6**	**7**	**8**
Demand - Capacity Ratio	1	1	1	1	1	1	1	1
Column & Beam (SB)	**1**	**2**	**3**	**4**	**5**	**6**	**7**	**8**
Demand - Capacity Ratio	0.98	1	1	1	1	1	0.9	0.9
Column & Beam (RB and IRB)	**1**	**2**	**1**	**2**	-			
Demand - Capacity Ratio	1	1	1	1				

Improving the manufacturing efficiency of tall building design depends on a number of factors, one of the most important of which is the stability of the columns. Sturdy columns are crucial to the stability and safety of tall buildings because they bear the weight of the building's vertical load. Designing tall buildings with weak beams can improve production efficiency without compromising safety. In order to save both time and resources, weak beams are often made with a smaller cross-section than primary beams. Table 3 and Figure 6 illustrate the inter-storey SC/WB ratio pertaining to the optimal design considerations for the 35-storey building.

Table 3. Drift Ratio for 35-Storey Building.

Columns (OC)	**1**	**2**	**3**	**4**	**5**	**6**	**7**	**8**
SC/WB Ratio	0.05	0.1	0.15	0.2	0.3	0.4	0.5	1
Columns (E2C)	**1**	**2**	**3**	**4**	**5**	**6**	**7**	**8**
SC/WB Ratio	1	1	1	1	1	1	1	1
Columns (E1C)	**1**	**2**	**3**	**4**	**5**	**6**	**7**	**8**
SC/WB Ratio	0.9	1	1	1	1	1	1	1

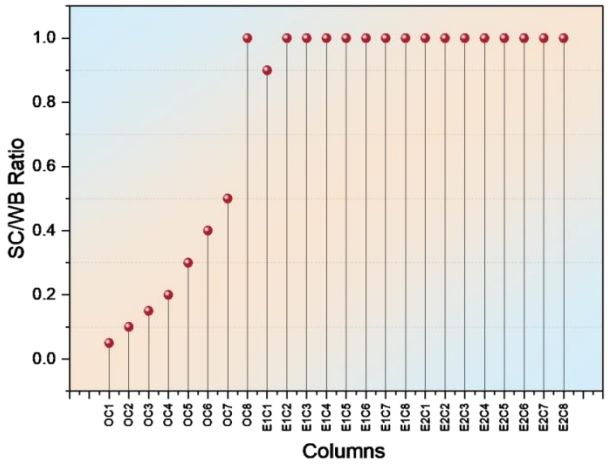

Figure 6. SC/WB ratio for 35 Storey Building

We evaluate the Manufacturing cost of the proposed method in tall building design by comparing it with other methods, such as the Tabu search algorithm (TS) [27] and Evolutionary structural optimization (ESO) [28].

The optimization of manufacturing efficiency for tall building design necessitates the implementation of a range of tactics and technologies with the objective of rationalizing the construction process and reducing expenses. The optimization of many components of the construction process is crucial in order to mitigate the substantial manufacturing costs associated with tall structure design. Figure 7 shows the comparison of manufacturing costs.

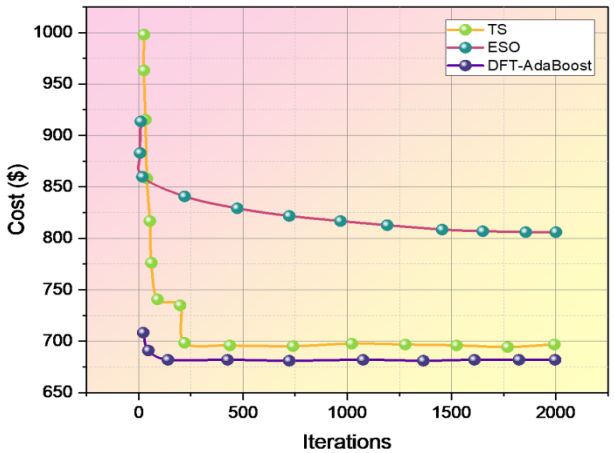

Figure 7. Comparison manufacturing cost

Improving tall building design manufacturing efficiency is a multifaceted process, and attaining the intended gains requires precise measurement. It is crucial to remember that the term "accuracy" can have several connotations and uses based on the particular context of tall structure design and construction procedures. Table 4 and Figure 8 show the accuracy of the tall building design.

Table 4. Accuracy for tall building design.

Epoch	**Accuracy (%)**
1	91
2	95.5
3	96.5
4	97.4
5	97.2
6	98
7	98.4
8	98
9	98.2
10	98.8

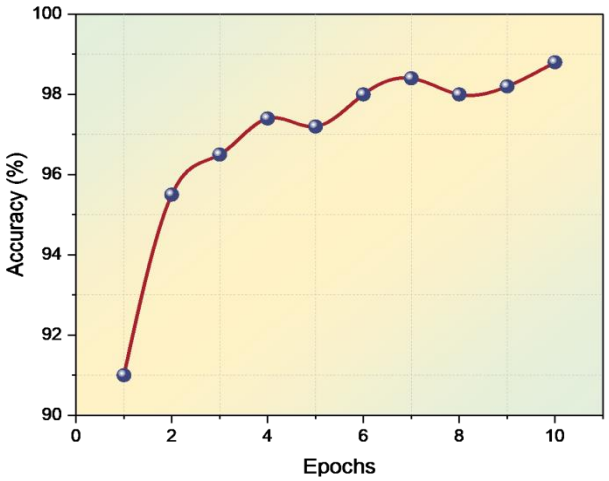

Figure 8. Accuracy for tall building design

6. CONCLUSION

Building skyscrapers has become a common sight in modern cities during a period of rapid urbanization and increasing demand for sustainable infrastructure. We presented a novel approach to overcome the shortcomings of traditional tall building design methodologies: dynamic

firefly-tuned AdaBoost (DFT-AdaBoost). The objective was to improve the sustainability and safety aspects of tall building design while simultaneously increasing manufacturing efficiency. Iteratively, the DFO was used to change different design factors, such as material types, sizes, and forms. Conversely, AdaBoosting is employed to enhance the model's projected accuracy. This methodology's iterative nature makes it possible to continuously enhance design solutions and achieve the required level of manufacturing efficiency. The study's conclusions showed significant improvements in manufacturing efficiency with regard to tall building construction. Reducing material waste and manufacturing costs can be achieved by identifying optimal design parameters through the application of the DFT-AdaBoost approach. When weak classifiers are overly complex, AdaBoosting may overfit, which reduces performance and makes it more vulnerable to outliers and noisy data. We want to develop an innovative method in the future to address these restrictions.

References:

Cruz, C. and Miranda, E., 2017. Evaluation of damping ratios for the seismic analysis of tall buildings. *Journal of Structural Engineering*, *143*(1), p.04016144. https://doi.org/10.1061/(ASCE)ST.1943-541X.0001628

De Domenico, D., Qiao, H., Wang, Q., Zhu, Z. and Marano, G., 2020. Optimal design and seismic performance of Multi-Tuned Mass Damper Inerter (MTMDI) applied to adjacent high-rise buildings. *The Structural Design of Tall and Special Buildings*, *29*(14), p.e1781. https://doi.org/10.1002/tal.1781

Elias, S. and Matsagar, V., 2018. Wind response control of tall buildings with a tuned mass damper. *Journal of Building Engineering*, *15*, pp.51-60. https://doi.org/10.1016/j.jobe.2017.11.005

Elshaer, A., Bitsuamlak, G. and El Damatty, A., 2017. Enhancing wind performance of tall buildings using corner aerodynamic optimization. *Engineering Structures*, *136*, pp.133-148. https://doi.org/10.1016/j.engstruct.2017.01.019

Elshaer, A., Gairola, A., Adamek, K. and Bitsuamlak, G., 2017. Variations in wind load on tall buildings due to urban development. *Sustainable cities and society*, *34*, pp.264-277. https://doi.org/10.1016/j.scs.2017.06.008

Gan, V.J., Chan, C.M., Tse, K.T., Lo, I.M. and Cheng, J.C., 2017. A comparative analysis of embodied carbon in high-rise buildings regarding different design parameters. *Journal of Cleaner Production*, *161*, pp.663-675. https://doi.org/10.1016/j.jclepro.2017.05.156

Gan, V.J., Cheng, J.C., Lo, I.M. and Chan, C.M., 2017. Developing a CO2-e accounting method for quantification and analysis of embodied carbon in high-rise buildings. *Journal of Cleaner Production*, *141*, pp.825-836. https://doi.org/10.1016/j.jclepro.2016.09.126

Gan, V.J., Deng, M., Tse, K.T., Chan, C.M., Lo, I.M. and Cheng, J.C., 2018. Holistic BIM framework for sustainable low carbon design of high-rise buildings. *Journal of Cleaner Production*, *195*, pp.1091-1104. https://doi.org/10.1016/j.jclepro.2018.05.272

Ghazali, A., Haw, L.C., Mat, S. and Sopian, K., 2017. Performance and financial evaluation of various photovoltaic vertical facades on high-rise buildings in Malaysia. *Energy and Buildings*, *134*, pp.306-318. https://doi.org/10.1016/j.enbuild.2016.11.003

Ierimonti, L., Caracoglia, L., Venanzi, I. and Materazzi, A.L., 2017. Investigation on life-cycle damage cost of wind-excited tall buildings considering directionality effects. *Journal of Wind Engineering and Industrial Aerodynamics*, *171*, pp.207-218. https://doi.org/10.1016/j.jweia.2017.09.020

Ji, X., Cheng, X., Jia, X. and Varma, A.H., 2017. Cyclic in-plane shear behavior of double-skin composite walls in high-rise buildings. *Journal of Structural Engineering*, *143*(6), p.04017025. https://doi.org/10.1061/(ASCE)ST.1943-541X.0001749

Li, QS, Li, X., He, Y. and Yi, J., 2017. Observation of wind fields over different terrains and wind effects on a super-tall building during a severe typhoon and verification of wind tunnel predictions. *Journal of Wind Engineering and Industrial Aerodynamics*, *162*, pp.73-84. https://doi.org/10.1016/j.jweia.2017.01.008

Li, Y., Tian, X., Tee, KF, Li, QS and Li, YG, 2018. Aerodynamic treatments for reduction of wind loads on high-rise buildings. *Journal of Wind Engineering and Industrial Aerodynamics*, *172*, pp.107-115. https://doi.org/10.1016/j.jweia.2017.11.006

Liew, J.Y.R., Chua, Y.S. and Dai, Z., 2019, October. Steel concrete composite systems for modular construction of high-rise buildings. In *Structures* (Vol. 21, pp. 135-149). Elsevier. https://doi.org/10.1016/j.istruc.2019.02.010

Lou, H., Gao, B., Jin, F., Wan, Y. and Wang, Y., 2021. Shear wall layout optimization strategy for high-rise buildings based on conceptual design and data-driven tabu search. *Computers & Structures*, *250*, p.106546. https://doi.org/10.1016/j.compstruc.2021.106546

Lou, H.P., Ye, J., Jin, F.L., Gao, B.Q., Wan, Y.Y. and Quan, G., 2021, December. A practical shear wall layout optimization framework for the design of high-rise buildings. In *Structures* (Vol. 34, pp. 3172-3195). Elsevier. https://doi.org/10.1016/j.istruc.2021.09.038

Lu, Z., Wang, D. and Zhou, Y., 2017. Experimental parametric study on wind-induced vibration control of particle tuned mass damper on a benchmark high-rise building. *The Structural Design of Tall and Special Buildings*, *26*(8), p.e1359. https://doi.org/10.1002/tal.1359

Meng, F.Q., He, B.J., Zhu, J., Zhao, D.X., Darko, A. and Zhao, Z.Q., 2018. Sensitivity analysis of wind pressure coefficients on CAARC standard tall buildings in CFD simulations. *Journal of Building Engineering*, *16*, pp.146-158. https://doi.org/10.1016/j.jobe.2018.01.004

Micheli, L., Hong, J., Laflamme, S. and Alipour, A., 2020. Surrogate models for high performance control systems in wind-excited tall buildings. *Applied Soft Computing*, *90*, p.106133. https://doi.org/10.1016/j.asoc.2020.106133

Oh, B.K., Kim, K.J., Kim, Y., Park, H.S. and Adeli, H., 2017. Evolutionary learning based sustainable strain sensing model for structural health monitoring of high-rise buildings. *Applied Soft Computing*, *58*, pp.576-585. https://doi.org/10.1016/j.asoc.2017.05.029

Pan, W. and Hon, C.K., 2020, June. Briefing: Modular integrated construction for high-rise buildings. In *Proceedings of the Institution of Civil Engineers-Municipal Engineer* (Vol. 173, No. 2, pp. 64-68). Thomas Telford Ltd. https://doi.org/10.1680/jmuen.18.00028

Petrini, F., Giaralis, A. and Wang, Z., 2020. Optimal tuned mass-damper-inerter (TMDI) design in wind-excited tall buildings for occupants' comfort serviceability performance and energy harvesting. *Engineering Structures*, *204*, p.109904. https://doi.org/10.1016/j.engstruct.2019.109904

Shen, W., Zhu, S., Xu, Y. L., & Zhu, H. P. 2018. Energy regenerative tuned mass dampers in high-rise buildings. *Structural Control and Health Monitoring*, *25*(2), e2072. https://doi.org/10.1002/stc.2072

Tomei, V., Imbimbo, M. and Mele, E., 2018. Optimization of structural patterns for tall buildings: The case of diagrid. *Engineering Structures*, *171*, pp.280-297. https://doi.org/10.1016/j.engstruct.2018.05.043

Tong, Z., Chen, Y. and Malkawi, A., 2017. Estimating natural ventilation potential for high-rise buildings considering boundary layer meteorology. *Applied energy*, *193*, pp.276-286. https://doi.org/10.1016/j.apenergy.2017.02.041

Venanzi, I., Lavan, O., Ierimonti, L. and Fabrizi, S., 2018. Multi-hazard loss analysis of tall buildings under wind and seismic loads. *Structure and Infrastructure Engineering*, *14*(10), pp.1295-1311. https://doi.org/10.1080/15732479.2018.1442482

Wang, S. and Mahin, S.A., 2018. High-performance computer-aided optimization of viscous dampers for improving the seismic performance of a tall building. *Soil Dynamics and* Earthquake Engineering, 113, pp.454-461. https://doi.org/10.1016/j.soildyn.2018.06.008

Weerasuriya, A.U., Zhang, X., Gan, V.J. and Tan, Y., 2019. A holistic framework to utilize natural ventilation to optimize energy performance of residential high-rise buildings. *Building and environment*, *153*, pp.218-232. https://doi.org/10.1016/j.buildenv.2019.02.027

Ashuvendra Singh
Dev Bhoomi Uttarakhand University, Dehradun, India
Pc.ce@dbuu.ac.in

Sandeep Singh Rawat
Dev Bhoomi Uttarakhand University, Dehradun, India
sandeep123.sr2@gmail.com

Navneet Kumar
Dev Bhoomi Uttarakhand University, Dehradun, India
navneetkumar97190@gmail.com